Title

Purification of Residual Ni and Co Hydroxides from Fe-Free Alkaline Electrolyte for Electrocatalysis Studies

Journal

ChemElectroChem, 9(15)

ISSN

2196-0216

Authors

Liu, Lu

Twight, Liam P

Fehrs, Jessica L

et al.

Publication Date

2022-08-12

DOI

10.1002/celc.202200279

Peer reviewed

Purification of residual Ni and Co hydroxides from Fe-free alkaline electrolyte for electrocatalysis studies

Lu Liu[a,b,†], Liam P. Twight[b,†], Dr. Jessica L. Fehrs[b], Yingqing Ou[b,c], Prof. Deen Sun[a,*] and Prof. Shannon W. Boettcher[b,*]

[a] School of Materials Science and Engineering, Chongqing University, Chongqing 400044, China

[b] Department of Chemistry and Biochemistry and the Oregon Center for Electrochemistry, University of Oregon, Eugene, Oregon 97403, United States

[c] School of Chemistry and Chemical Engineering, Chongqing University, Chongqing 400044, China

[†] These authors contributed equally to this work.

AUTHOR INFORMATION

Corresponding Author

* Deen_Sun: Deen_sun@cqu.edu.cn

* Shannon W. Boettcher: swb@uoregon.edu **Web:** boettcher@uoregon.edu Twitter: @BoettcherLab

Notes

The authors declare no competing financial interest.

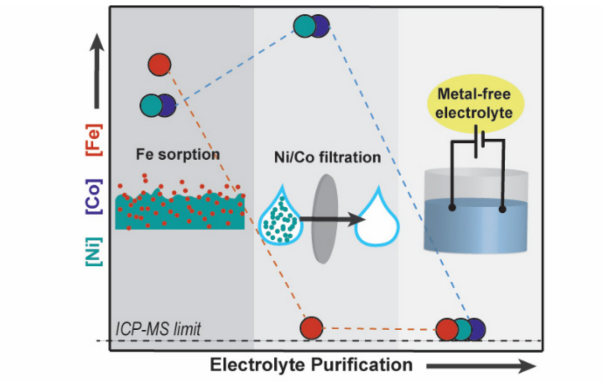

Table of contents: $Ni(OH)_2$ and $Co(OH)_2$ sorbents remove Fe impurities from alkaline electrolyte used for oxygen evolution electrocatalysis but leave behind $Ni(OH)_2$ and $Co(OH)_2$ residues. We show that simple (nano)filtration removed residues faster and more-completely than time-consuming electrolysis, down to a few parts-per-billion, as determined by cyclic voltammetry and inductively coupled plasma mass spectrometry, providing clean electrolyte for fundamental studies.

Abstract: It is critical to control Fe impurity concentrations in oxygen-evolution-reaction electrocatalysis experiments so that unambiguous assignments of activity and mechanistic details can be made. An established method to prepare Fe-free KOH electrolyte is by using particulate $Ni(OH)_2$ or $Co(OH)_2$ as absorbents to remove the Fe from KOH or other neutral-to-alkaline electrolytes. However, this method yields residual Ni or Co species in the electrolyte which can be redeposited on the working electrode. Thus, current methods of Fe removal could convolute studies of OER. In this work, we compared two different methods, continuous electrolysis and nano-filtration, to remove the Ni and/or Co species from Fe-free alkaline electrolyte. We found the best approach is to pass the Fe-free electrolyte through a hydrophilic 0.1 μm polyethersulfone filter which decreases the Ni species concentration in 1 M KOH to single ppb levels. This result suggests the remaining Ni or Co species are primarily particulate in nature, consistent with their small solubility as ions. In comparison, extended pre-electrolysis of the electrolyte removed only a portion of the Ni/Co.

Key words: oxygen evolution reaction, electrocatalysis, Fe impurities, Ni(Co) precipitates, KOH purification

Introduction

Water electrolysis using renewable electricity is a promising route to produce clean renewable hydrogen. However, slow oxygen-evolution-reaction (OER) kinetics limit electrolyzer performance, and it remains a challenge to discover inexpensive OER catalysts with both high activity and long-term stability.[1-4] Materials based on abundant first-row transition metals like Fe, Ni, and Co are among the most promising with some already used in commercial alkaline electrolyzers.[5-8]

Nickel (oxy)hydroxide in particular has been studied for decades as a high-activity OER catalyst in alkaline conditions.[9-11] Studies by Corrigan in the 1980s[12] revealed that this high activity is realized when Fe impurities are present in electrolyte at sub-ppm or higher levels. More recently, it was found that the intrinsic activity of Ni and Co (oxy)hydroxide is roughly 1000- and 30-times higher after Fe impurity incorporation compared to their rigorously Fe-free forms.[13-15] Soluble Fe impurities also enhance the performance of catalysts in near-neutral conditions.[16] Markovic and co-workers reported that Fe-based surface active sites are dynamically stable as a result of dissolution and re-deposition at the electrolyte/host interface.[17,18] While the role of absorbed Fe species[19,20] has not been rigorously studied for many other OER catalyst types, such as perovskite oxides,[18,21,22] it is almost certainly important in these as well. Broadly, there is a tremendous quantity of published and ongoing work on metal oxides/(oxy)hydroxide[23,24] water oxidation catalysts in which the role of electrolyte Fe species is of obvious,[25,26] but not universally appreciated,[27,28] importance.

Given these considerations, any mechanistic or intrinsic-activity study of OER in neutral to alkaline conditions needs to be done in electrolytes free from Fe impurities. Generally, three methods have been used to remove the unwanted Fe from alkaline electrolytes (such as 1.0 M KOH). One is removing the Fe by prolonged electrolysis for which there is well-established precedent in the literature. Spanos et al. reported purification of KOH by electrolysis with NiS_3–MoS_2 catalyst as both working and counter electrode under a current of 100 mA for 12 h.[29] Chung and coworkers removed Fe by prolonged electrolysis for five days using a Ni wire as both working and counter electrode.[17] Both studies illustrate the electrolysis approach is time-consuming, likely due to the need for transport of Fe species to an electrode of finite size. Ion-exchange resins have also been used to purify KOH electrolyte. In one case, Chen et al. purified the electrolyte of Fe using Amberlite IRC748 resin, a chelating iminodiacetic-acid cation-exchange resin.[30] In this case, residual organic species may enter the electrolyte from the resin. We previously adopted a method that uses high-purity nickel or cobalt hydroxide powders to absorb soluble Fe species from neutral-to-alkaline electrolytes[10] and this method has been adopted by many others for the purification of alkaline electrolytes. The weakness of this method, as we discussed earlier,[31] is that it leaves residual Ni or Co hydroxides in the purified electrolytes. Despite not being a major issue when testing the intrinsic activities of Ni or Co (oxy)hydroxides (assuming the electrolyte is purified with the same metal hydroxide as under test as a catalyst), the existence of these residues could complicate studies of catalysts of different composition. For example, materials such as transition-metal chalcogenides and phosphides have been reported to have high OER activity, but the state of the surface during OER is complex. Co or Ni residues could introduce ambiguity in surface characterization and correlation of structure to activity.[32-34] $Ni(OH)_2$ deposits also pose a risk of erroneous measurements of the hydrogen evolution reaction (HER) on platinum because of its apparent catalytic enhancement in alkaline conditions.[35]

Here we compare the effectiveness of two methods to remove residual Ni and Co hydroxide species from alkaline electrolyte. We show that simply filtering the electrolyte though nanoporous syringe filters is sufficient to remove Ni to near the detection limit of our inductively coupled plasma mass spectrometry (ICP-MS) system in KOH – a degree of removal that prolonged electrolysis is unable to easily attain. We report the effects of filter pore size and filter hydrophilicity on the removal efficacy. Based on elemental analysis by ICP-MS and by testing the electrolytes under practical OER test conditions, we conclude that using a 0.1 μm hydrophilic polyethersulfone (PES) filter after Fe adsorption by Ni or Co hydroxide powder, centrifugation, and decanting, reproducibly provides for the cleanest alkaline electrolytes for OER tests. Because filtration through a 0.1 μm filter cannot remove soluble metal ions, these results also show that the soluble ion concentration is quite low and the primary Ni or Co contaminant in these systems are particulate/colloidal in nature.

Results and discussion

After purification of KOH electrolyte using the $Ni(OH)_2$ or $Co(OH)_2$ absorption method, the concentrations of residual Ni and Co were measured by ICP-MS. The concentration of Fe in all solutions were below the limit of detection of 2.0 ppb and so the method of standard additions was employed, the results of which are discussed below. The equilibrium solubilities of Ni^{2+} at pH 13 and 14 are calculated to be roughly 0.1 ppm and 0.4 ppm, respectively.[36] ICP-MS results are shown in Table 1. The concentration of Ni in 0.1 M KOH and 1.0 M KOH solution is 1.4 ± 1.0 and 3.4 ± 3 ppm, respectively. Note that these are not related by a factor of 10 as expected from dilution. This could be due to adsorption of some of the species to the walls of the container. Similar concentrations of Co were shown in Co-cleaned Fe-free KOH. Significant levels of Ni and Co species are thus retained when using the corresponding hydroxides for Fe purification. These residual Ni or Co species exist most likely as particulates in addition to soluble species. We note that the amount of Ni or Co existing in KOH after Fe cleaning is variable and depends on Fe-Free KOH preparation details, such as, time and speed of centrifugation, the volume of KOH, the quantity of Ni or Co hydroxide and so on.

After establishing baseline levels of residual Ni and Co, we investigated the efficacy of their removal with extended electrolysis for 3 h at 2.0 V vs. Hg/HgO as well as via purification with syringe filters with different pore sizes. The degree of electrolyte purity after application of each method was first assessed by cyclic voltammetry.[31] Extended cycling reveals small waves associated with redox from NiO_xH_y or CoO_xH_y that had been deposited from the electrolyte, probably as particles, as well as broad redox pseudocapacitive features perhaps due surface-absorbed speices. Monitoring the integrated current density of these redox features thus serves as an approximate means of assessing the efficacy of Ni or Co removal.

Table 1. ICP-MS data of Fe-free KOH before and after further purification by electrolysis

Method of Fe cleaning	Ni (ppm)	Co (ppm)
Fe-free 0.1 M KOH cleaned with $Ni(OH)_2$	3.4 ± 1.0	--
Fe-free 10 mL 0.1 M KOH *after* 3 h electrolysis	1.4 ± 1.0	--
Fe-free 50 mL 0.1 M KOH *after* 3 h electrolysis	2.0 ± 1.0	--
Fe-free 1.0 M KOH cleaned with $Ni(OH)_2$	1.4 ± 1.0	--
Fe-free 10 mL 1.0 M KOH *after* 3 h electrolysis	0.7 ± 1.0	--
Fe-free 50 mL 1.0 M KOH *after* 3 h electrolysis	1.1 ± 1.0	--
Fe-free 0.1 M KOH cleaned with $Co(OH)_2$	--	0.8 ± 1.0
Fe-free 1.0 M KOH cleaned with $Co(OH)_2$	--	1.0 ± 1.0

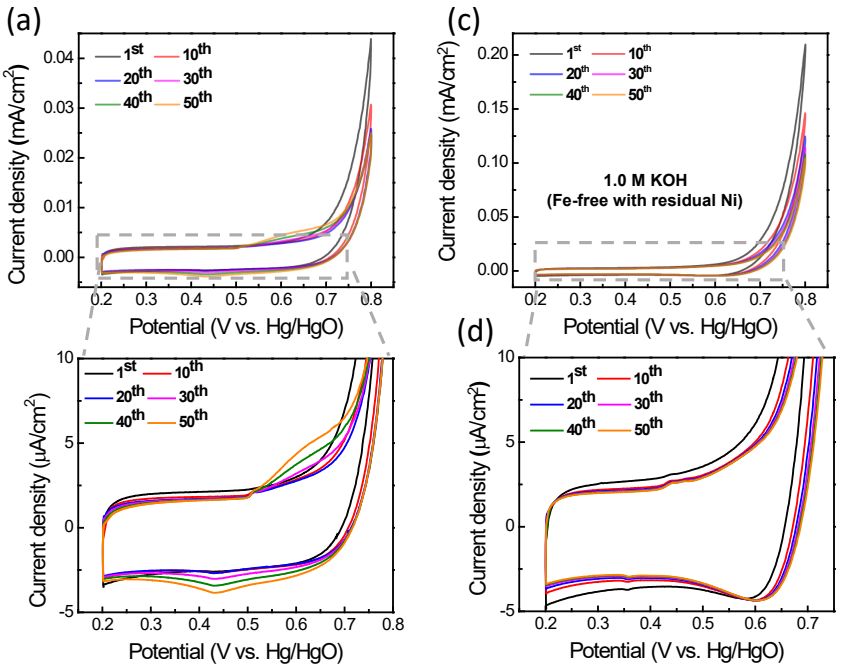

Figure 1. Cyclic voltammogram of Pt coils in $Ni(OH)_2$-cleaned Fe-free (a) 0.1 M , (c) 1.0 M KOH electrolyte; (b) and (d) show the corresponding enlarged precatalytic regions with the number referring to cycle number. The electrodes show different capacitive currents because of the different-sized Pt coils used in the tests. The surface area of the Pt-coil working electrode used is 1.8 cm^2 in 0.1 M KOH and 4.1 cm^2 in 1.0 M KOH. The growth of a redox wave associated with $Ni(OH)_2$/NiOOH redox is apparent upon extended cycling in 0.1 M KOH. The apparent redox wave from $Ni(OH)_2$/NiOOH appears largely on the first couple cycles for the 1.0 M KOH, which suggests that the $Ni(OH)_2$ colloids/particulates may absorb even in the absence of bias. The precatalytic $Ni(OH)_2$/NiOOH features, most notably the large cathodic feature, do disappear in the further cleaned electrolyte from which Ni impurities are removed (see below) for both electrolytes.

Figure 1 shows a series of voltammograms using Pt coils in Fe-free KOH purified using $Ni(OH)_2$. Small redox features attributed to NiO_xH_y redox located before the onset of OER are evident during cycling and increase with cycle number. This suggests that Ni residues are gradually depositing on the surface of the Pt coil in both 0.1 M and 1.0 M KOH even though ICP-MS indicates Ni is only present at the 1-3 ppm level. As shown in Figure 1a and 1b, the peak becomes observable after as few as 10 cycles. After 50 CV cycles, the peak current density reaches a maximum. Similar results were observed in 1.0 M KOH (Figure 1c and 1d). The peak was observed after 10 CV cycles and stabilizes with a height of ~3 μA/cm^2 after 50 CV cycles. This voltammetry, together with the ICP-MS results (Table 1), shows that Ni or Co species in KOH electrolyte are present after Fe cleaning and that these could interfere with mechanistic studies of OER processes as the Ni or Co can redeposit on the catalyst surface.

We next attempted the removal of the $Ni(OH)_2$ by prolonged electrolysis at 2.0 V vs Hg/HgO for 3 h using a two-electrode set up in 10 and 50 mL electrolyte cells under stirred conditions. The working and counter electrode were cleaned every hour using aqua regia to remove any species that had deposited on the cleaning electrodes. As shown in Figure 2a, the Ni redox peak was observed in the 50 mL electrolyte cell after 50 CV cycles. The redox peak height from Ni (oxy)hydroxide deposition after electrolysis in both the 10 and 50 mL cells were lower than for the Fe-free electrolyte that was not electrolyzed. Comparable results were obtained for the 1.0 M KOH (Figure 2b). Decreased peak height indicates a reduction of the amount Ni in the electrolyte due to the electrolysis step. The presence of a noticeable peak due to NiO_xH_y in the 50 mL electrolyte volume is likely because there is more residual Ni in the 50 mL volume to remove. Presumably longer electrolysis times would more-completely remove the $Ni(OH)_2$ in the larger electrolyte volume – although this can be a time-consuming process for larger electrolyte volumes.

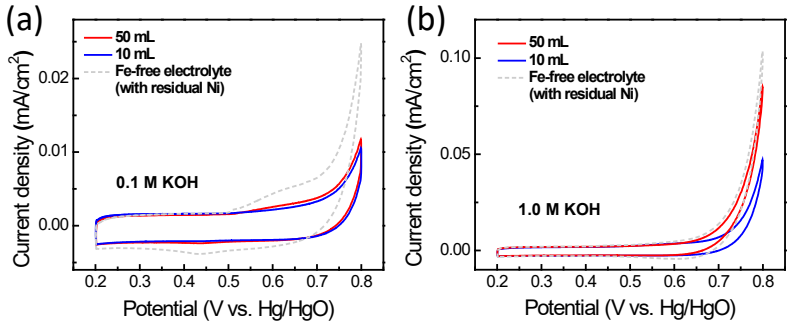

Figure 2. The 50th CV curves of Pt coils in Fe-free 0.1 M (a) and 1.0 M (b) KOH electrolyte after 3 h electrolysis at 2.0 V in 10 and 50 mL of electrolyte, respectively. Pt coils with surface areas of 1.8 cm^2 and 4.1 cm^2 were used for electrochemical measurements in 0.1 and 1.0 M KOH electrolyte, respectively. The OER currents are small and relatively similar across the samples with those measured for the nano-filtered electrolytes lower due to less $Ni(OH)_2$ deposition on the electrode surface during cycling.

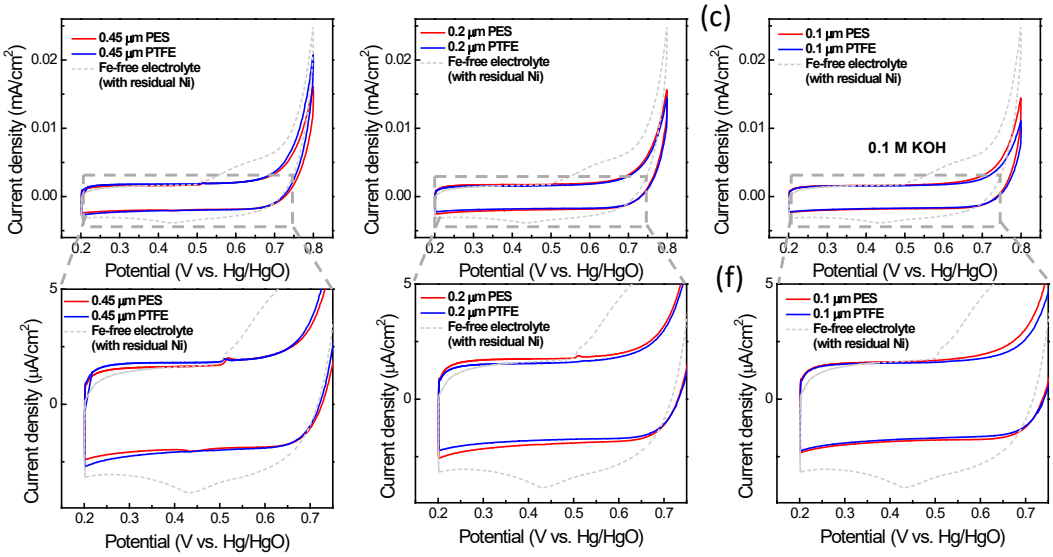

Figure 3. CV curves of a Pt coil (surface area 1.8 cm^2) after 50 CV cycles in 10 mL of Ni-cleaned Fe-free 0.1 M KOH using different pore size filters (a) and (d) 0.45 µm, (b) and (e) 0.2 µm, (c) and (f) 0.1 µm. PTFE was the hydrophobic filter material, and the PES was the hydrophilic filter material.

To compare to electrolysis, Ni purification was performed using hydrophobic and hydrophilic syringe filters with pore sizes of 0.45, 0.2, 0.1 µm. The KOH treated after filtration was collected and analyzed for residual metal species using cyclic voltammetry as above. Figures 3 and 4 show that filtration appears to remove Ni contamination left by the Fe adsorption step in both 0.1 M and 1.0 M KOH based on the decrease of redox peak sizes, pseudo-capacitive current, and OER current before and after filtration. The different shapes of the redox peaks, broader and larger in 0.1 M KOH compared to 1.0 M KOH, could be due to differences in the details of Ni residue adsorption to the Pt coil. The lowest Pt OER current densities at a given overpotential are obtained by using the 0.1 µm pore-size filter for both 0.1 M and 1.0 M KOH which, which is discussed further below.

For a given pore size, the efficacy of metals removal does not obviously depend on filter hydrophobicity. For example, the pre-catalytic feature associated with NiO_xH_y is more prominent for the 0.2 µm PTFE filter for 1.0 M KOH (Fig. 4b), but not

in 0.1 M KOH (Fig. 3b). The hydrophobic PTFE filter, however, is much more difficult to pass the aqueous electrolyte through, especially at the 0.1 µm pore size, so the PES filter is recommended.

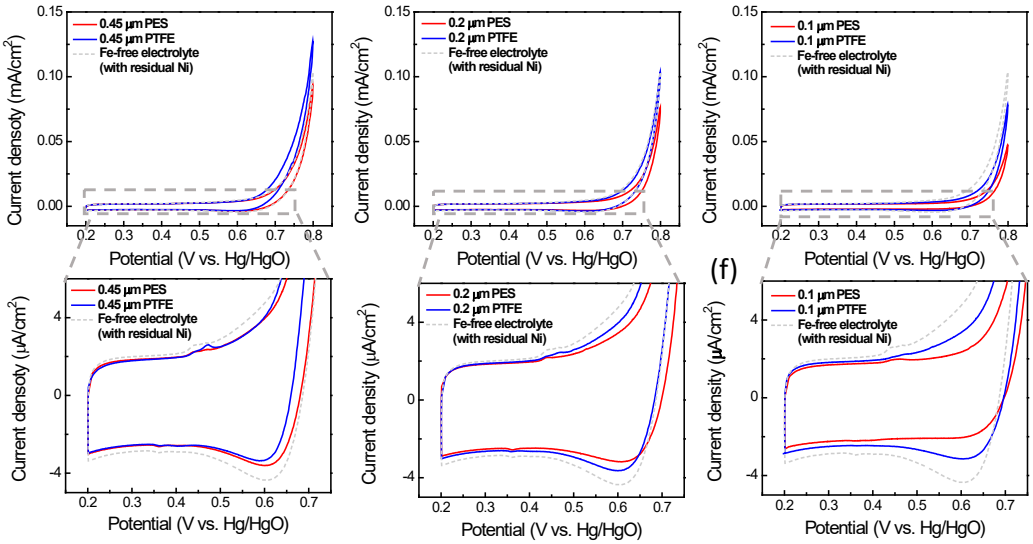

Figure 4. CV curves of Pt coil with surface area 4.1 cm^2 at 50th cycle in 10 mL of Ni-cleaned Fe-free 1 M KOH after filtering through different pore sizes (a) and (d) 0.45 µm, (b) and (e) 0.2 µm, (c) and (f) 0.1 µm.

Like Ni, residual Co species deposited as CoO_xH_y on the surface of the working electrode can be assessed by the size of its redox features around 0.25 V *vs.* Hg/HgO. The data in Figure 5 shows there is significantly more residual Co in the 1.0 M KOH than the 0.1 M KOH cleaned with the $Co(OH)_2$. This may simply be because of the variable nature of how much $Co(OH)_2$ sorbent is transferred during electrolyte processing or as a result of different particle-size distribution of $Co(OH)_2$ in the 0.1 M KOH which happen to be more difficult to deposit at the working electrode. The 0.1 µm PES hydrophilic filter was used to remove the Co species in the KOH. As shown in Figure 6a and 6b, there is no peak observed after 50 CV cycles in 0.1 M and 1.0 M KOH which indicates good performance for the removal of CoO_xH_y species from the Fe-free electrolyte.

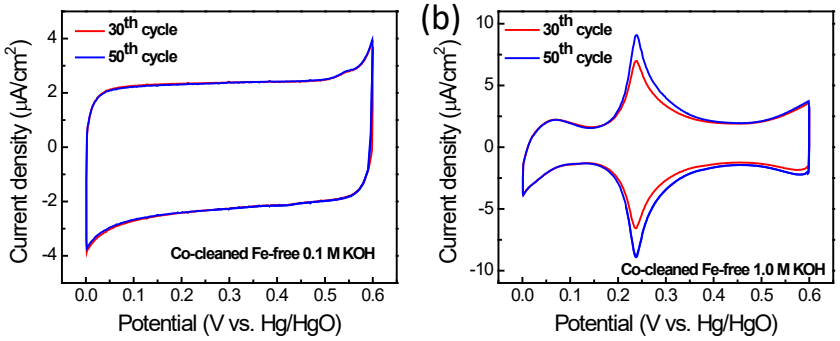

Figure 5. Cyclic voltammogram of Pt coils in Co-cleaned Fe-free 0.1 M (a) and 1.0 M (b) KOH electrolyte (10 mL each). The surface area of the Pt coil working electrode used is 1.8 cm^2 in 0.1 M KOH and 4.1 cm^2 in 1.0 M KOH.

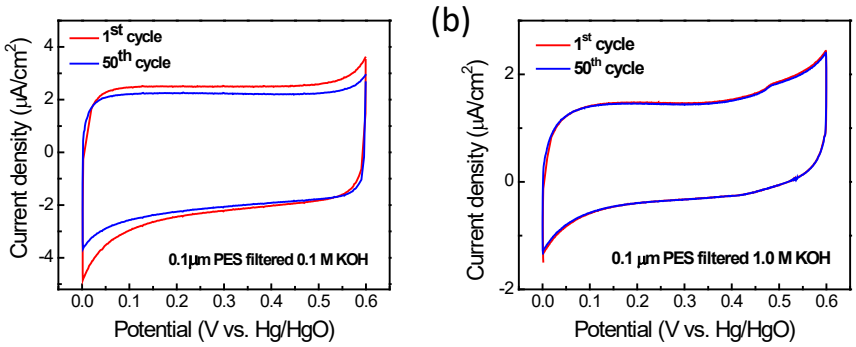

Figure 6. Cyclic voltammogram of Pt coil in Co-cleaned after 0.1 um PES filter 0.1 M (a) and 1.0 M (b) KOH electrolyte (10 mL each). The surface area of the Pt coil working electrode used is 1.8 cm^2 in 0.1 M KOH and 4.1 cm^2 in 1.0 M KOH.

To complement cyclic voltammetry, we used ICP-MS to quantify the amount of Fe, Ni or Co in the Fe-free electrolyte after purification. We found that the measured analyte signal (counts pers second – cps) assigned to Ni, Co, and Fe, was lower than that of the blank prepared from semiconductor-grade KOH neutralized with nitric acid (trace-metal grade). Although this indicated that the scrubbing/nanofiltration purification protocol developed here lowers significantly not only the Fe impurity levels, but also the Ni and Co impurity levels, compared to the best-available grade KOH, it also necessitated a different approach to quantification.

The signal intensities of the analytes in the $Ni(OH)_2$ cleaned and filtered samples were below the detection limit set by the nominally 0 ppb blank because matrix matching was achieved in the calibration standards using relatively lower purity semiconductor grade KOH. We therefore quantified the Fe, Ni, and Co amounts using the method of standard additions. A standard additions curve was constructed by spiking small aliquots of a solution continuing Fe, Ni, and Co of known concentration into 1.0 M KOH cleaned using a 0.1 μm PTFE filter. The concentration of species was obtained by extrapolating the linear curve fit to the x-axis or equivalently, the ratio of the intercept to the slope.[37] We note that the method of standard additions assumes similar matrix effects among all samples and negligible instrument drift during sample measurement. Only one filtration condition and KOH concentration was used to generate the curve because quantities of Fe, Ni, and Co in 0.1 M KOH can be simply related to 1.0 M KOH by a dilution factor of 10. The concentrations in the unknown sample serving as the lowest standard were determined by linear extrapolation. The concentrations of Fe, Ni, and Co in the remaining filtered 1.0 M KOH samples were determined by dividing the measured intensities of each element by the slope of the standard additions curve. The results of this standard addition approach are depicted in Figure 7 for Fe, Ni, and Co and the concentrations for each sample reported in Table 2.

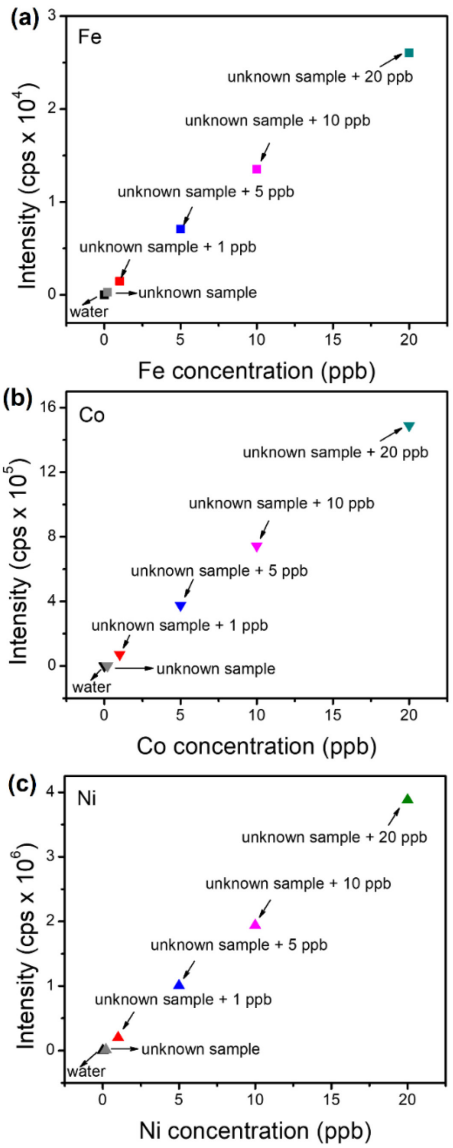

Figure 7. ICP-MS calibration curves for (a) Fe, (b) Co and (c) Ni. The unknown sample represents the 1.0 M Fe-free KOH electrolyte cleaned by the 0.1 μm PTFE filter.

Table 2. ICP-MS results of 1.0 M Fe-free KOH after purification by filtering

Samples	Fe (ppb)	Ni (ppb)	Co (ppb)
Blank solution 1.0 M semiconductor KOH[a]	17 ± 2	36 ± 1	0.53 ± 0.07
Ni-cleaned Fe-Free KOH (no filtration)	6.5 ± 0.7	57 ± 2	0.38 ± 0.04
0.45 μm PTFE[b]	12 ± 2	2.7 ± 0.3	0.68 ± 0.02
0.2 μm PTFE[b]	7.2 ± 1.0	2.2 ± 0.1	0.56 ± 0.07
0.1 μm PTFE[c]	7.3 ± 1.6	2.5 ± 0.1	0.56 ± 0.04
0.45 μm PES[b]	8.5 ± 0.9	2.5 ± 0.1	0.47 ± 0.06
0.2 μm PES[b]	7.9 ± 0.6	4.6 ± 0.3	0.59 ± 0.06
0.1 μm PES[b]	9.2 ± 1.2	2.3 ± 0.1	0.60 ± 0.05

[a] 350 μL 1.0 M KOH untreated, neutralized with 5 % vol. HNO_3 to 10.0 mL.
[b] Here 350 μL 1.0 M KOH electrolyte purified by absorption of Fe onto $Ni(OH)_2$ followed by nanofiltration and neutralized with 5 % vol. HNO_3 to 10.0 mL.
[c] the filtration condition used to generate the unknown whose concentration is found by extrapolation of the standard addition curve to the x-axis.

Use of the $Ni(OH)_2$ sorbent increased the amount of Ni in the as-prepared semiconductor-grade 1.0 M KOH electrolyte from 36 ppb to ~ 57 ppb. Filtration generally removed both Ni present from the dissolved KOH pellets and that introduced in the Fe-purification to a level of 2-3 ppb regardless of pore size and hydrophilicity – a removal efficacy of ~95%. We note that the amount of Ni present after Fe purification is sensitive to how the experimentalist pours off the Fe-free supernatant after centrifugation (and thus the quantity of retained $Ni(OH)_2$ particulates), so this quantity is difficult to control and thus probably variable across different batches. We suggest that because the Ni present after Fe-purification is particulate in nature, the amount of Ni before purification varies, and that large volumes are easily processed by filtration, that filtration generally outperforms electrolysis for removal.

According to Table 2, the concentration of Fe after treatment of the 1.0 M KOH with $Ni(OH)_2$ sorbent was roughly 10-fold lower than the as-prepared electrolyte and that this does not change regardless of the filter used during Ni filtration. There did seem to be Fe introduced into the sample above the baseline Fe-cleaned electrolyte during filtration with the 0.45 μm PTFE filter, highlighting the challenge of preventing contamination from Fe in the laboratory environment. Because the presence of Fe is responsible for orders-of-magnitude increase in activity in Co- and Ni oxide catalysts,[10,15] this 10-fold reduction in Fe has significant impacts on measurements of their intrinsic activity. The measured amount of Co is very low in all samples, treated or untreated.

The signal intensities of Fe, Ni, and Co in analogously treated 0.1 M KOH were also measured with ICP-MS but are not reported here. Quantification using the curve found by standard additions based on 1.0 M KOH dilution would not be appropriate because of differing matrix effects. That said, the signal intensities can be used to make a qualitative assessment of Fe, Ni, and Co levels. Signal intensity for Fe seemed to indicate that the amount of Fe is lower in the 0.1 M KOH relative to 1.0 M KOH, as one would expect from dilution, although this was by about a factor of two rather than by ten. In other words, more-modest reduction of Fe can be expected by treating 0.1 M KOH than 1.0 M KOH. Ni signal intensity was 10-fold higher in the 0.1 M KOH after Fe-purification only than in 1.0 M KOH, but post-filtration intensities were comparable, supporting the idea that filtration reduces the amount of Ni to roughly the same concentrations regardless of initial concentration after Fe sorption. Co intensities remained low and unchanging across all conditions.

Together, the data suggest that purification of electrolyte for alkaline OER electrocatalysis experiments is especially important when performed in 1.0 M KOH in which the Fe concentration is higher than in 0.1 M KOH. Comparatively, 0.1 M

semiconductor grade KOH seems to be dilute enough that it is near the purity level achievable by Fe sorption. We note that the magnitude of the cathodic wave at ~ 0.6 V vs Hg|HgO, assigned to the reduction of surface-absorbed NiOOH, observed in 1.0 M KOH electrolyte filtered through 0.1 μm pores, is much smaller than for the larger filters. In comparison, there is very little change in the same cathodic wave when the 0.45 um filter is used (compare Figure 4d and 4f). The magnitude of the OER current is also minimized through the use of the 0.1 um PES filter, relative to the other larger filters. For the 0.1 M KOH case, the difference in filter efficacy is less obvious from changes in the Ni redox wave, however, when the 0.45 um filter was used a small positive wave at ~ 0.47 V vs Hg|HgO is evident, and such waves are not observed when the 0.1 um PES filter is used. Likely, these peaks, reminiscent of those due to well-formed $Ni(OH)_2$, are due to entire $Ni(OH)_2$ particles that have attached to the surface from the electrolyte. The 0.1 um PES filter also provided for the lowest OER current in 0.1 M KOH. Finally, we note that all the ICP-MS data for the 1.0 M KOH shows similar, very small, amounts of residual Ni in the filtered electrolyte. It is possible that the $Ni(OH)_2$ electrolyte treatment, followed by filtering, removes additional species that modulate the (low) measured OER activities here. In any case, these analyses lead us to be confident in recommending the smallest hydrophilic filter, 0.1 μm PES, for electrolyte cleaning.

Conclusion

Cleanliness of an electrolyte is essential for rigorous measurement of OER electrocatalyst properties in alkaline media yet is often overlooked. We compared removal of Ni and Co species from Fe-free alkaline electrolyte using two methods, multi-hour electrolysis and nano-filtration. Prolonged electrolysis removes a large fraction of residual Ni species but is not as effective as nanofiltration, for which metal levels were reduced to single digit ppb levels. We also found from evaluating electrochemical features that the extent of purification of the Co and Ni species (presumably nanoparticulates) was inversely correlated to the filter pore size although this was less obvious in ICP-MS data. ICP-MS measurements further suggested that intrinsic catalytic activities measured in semiconductor grade 1.0 M KOH prepared without further purification are more likely to suffer from extrinsic influences i.e. soluble Fe species. Comparatively, 0.1 M semiconductor grade KOH seems to be dilute enough that it is already near (though not at) the Fe purity level achievable by Fe sorption. Filtration of Ni residue should be performed regardless of KOH concentration when $Ni(OH)_2$ is used as the Fe sorbent in a previous step. Ultimately, we find that sorption of trace Fe with a $Ni(OH)_2$ sorbent followed by filtration with a 0.1 μm PES filter yields the best combination of experimental practicality and purification efficacy for alkaline OER catalysis studies.

Experimental

Chemicals. We used potassium hydroxide hydrate (semiconductor grade, 99.99%, Sigma Aldrich), Ni nitrate hexahydrate (99.999% metal basis, Sigma Aldrich), Co nitrate hexahydrate (99.999%, Sigma Aldrich); cobalt, nickel, and iron ICP-MS standard (1000 ppm, Ricca); yttrium standard solution (1001 ± 1 ppm, Aristar), scandium standard (994 ± 6 ppm, Sigma Aldrich); and nitric acid (trace metal analysis grade, Aristar Plus). Electrolytes were prepared with 18.2 MΩ·cm deionized (DI) water.

Preparation of Fe-free KOH electrolyte. The 0.1 M and 1.0 M Fe-free KOH electrolyte was purified as described previously.[10] Here we describe the procedure using $Ni(OH)_2$ absorbents to remove Fe as an example. First, high-purity $Ni(OH)_2$ was prepared as follows: 2 g of 99.999% $Ni(NO_3)_2{\cdot}6H_2O$ were dissolved in 4 mL of 18.2 MΩ·cm H_2O in a H_2SO_4-cleaned 50 mL polypropylene centrifuge tube. 20 mL of 1.0 M KOH (semiconductor grade) were added to precipitate high-purity $Ni(OH)_2$. The mixture was shaken vigorously for at least 10 min and centrifuged for at least 10 min before decanting the supernatant. The prepared $Ni(OH)_2$ was then washed (two times) by adding 20 mL of 18.2 MΩ·cm water and 2 mL of 1.0 M

KOH to the centrifuge tube, re-dispersing the solid by shaking, centrifuging and decanting the supernatant. Finally, purification of the 0.1 M or 1.0 M KOH electrolyte was performed by redispersing the clean $Ni(OH)_2$ in 50 mL 0.1 M or 1.0 M KOH, shaking vigorously at least 10 min, and allowing the mixture to rest at least 3 h. After centrifugation, the purified Fe-free KOH supernatant was decanted into a H_2SO_4-cleaned polypropylene bottle for storage.

Ni-/Co-free and Fe-free KOH Electrolytes. For Ni-Free KOH electrolyte, two methods were used to purify the electrolyte. The first method was prolonged electrolysis. 10 or 50 mL of Fe-free KOH were electrolyzed using a two-electrode setup with stirring in a plastic (polypropylene) container covered with parafilm. Homemade platinum coil electrodes with surface areas of 1.8 cm^2 and 4.1 cm^2 served as the working and counter electrode. Another method for removing Ni species in Fe-free KOH electrolyte was filtration with syringe filters (hydrophobic Corning polytetrafluoroethylene or hydrophilic Acrodisc polyethersulfone) with pore sizes of 0.45, 0.2, and 0.1 μm and a diameter of 32 mm. After purification, the KOH solution was withdrawn to store in an acid-cleaned polypropylene bottle.

Electrochemical characterization. All electrochemical measurements were made using a BioLogic potentiostat (SP300) in a two-electrode mode (prolonged electrolysis) or three-electrode mode (cyclic voltammetry) with a Hg/HgO reference electrode (RE, CH Instruments, CHI152). Coiled Pt wire with surface area of 1.8 cm^2 or 4.1 cm^2 (3.15 mm diameter, 99.99%,) were used as the working and counter electrodes as this provides a redox-peak free and OER inert substrate that is therefore sensitive to adsorbed Ni and/or Fe residues. All alkaline electrochemical measurements were made in plastic (polypropylene) containers with “hot glue” (commonly available hot-melt polymer adhesive) used to fabricate the electrodes that are in contact with electrolyte. All electrochemical cell components were cleaned prior to experiments with 1 M H_2SO_4 and rinsed with 18.2 MΩ·cm water.

Elemental analysis. The quantity of Ni and Co in KOH solution was determined by inductively coupled plasma mass spectrometry (ICP-MS, iCAP-RQ Qnova Series, Thermo Fisher Scientific). To make calibration curves, the first step was to prepare the matrix for “matrix matching” between calibration curves and samples. For quantification of metals in KOH (1 M and 0.1 M) electrolyte, 350 μL of KOH was neutralized with 10.0 mL of 5 % by vol. HNO_3 to ensure solubility of metal ions and adherence to the <0.2% total dissolved solids (TDS) limit of the ICP-MS. Failure to account for this TDS restriction can lead to crystallization of KOH at the nebulizer tip and erroneous measurements. Next, commercial Ni, Co, and Fe reference solution (at 10 ppm) was added in an appropriate amount such that the standards contained 1, 5, 25, or 100 ppb in the matrix. Finally, internal standards Y and Sc were added into the solutions with a concentration of 25 ppb each. The samples solutions for analysis were prepared identically to the standard solutions – aliquots of electrolyte were diluted by 5 v/v% HNO_3 and then internal standard was added. Values in Table 1 were determined in this manner, those in Table 2 were found by the method of standard additions.

Acknowledgment

This work was supported by the National Science Foundation Chemical Catalysis Program, Award # 1955106. The ICP-MS instrument was funded by an NSF MRI Award #2117614. L.L. and Y.O. acknowledge support from the China Scholars Council.

Keywords:

electrocatalysis, electrolyte, impurities, iron, water oxidation

References

[1] G. Dey, Shadab, A. Aijaz, *ChemElectroChem* **2021**, *8*, 3782-3803.

[2] T. Noor, L. Yaqoob, N. Iqbal, *ChemElectroChem* **2021**, *8*, 447-483.

[3] I. Katsounaros, S. Cherevko, A. R. Zeradjanin, K. J. J. Mayrhofer, *Angew. Chem. Int. Ed.* **2014**, *53*, 102-121.

[4] R. A. Krivina, Y. Ou, Q. Xu, L. P. Twight, T. N. Stovall, S. W. Boettcher, *Acc. Mater. Res.* **2021**, *2*, 548-558.

[5] Y. Ou, W. Tian, L. Liu, Y. Zhang, P. Xiao, *J. Mater. Chem. A* **2018**, *6*, 5217-5228.

[6] L. Liu, Y. Ou, D. Gao, L. Yang, H. Dong, P. Xiao, Y. Zhang, *Journal of Power Sources* **2018**, *396*, 395-403.

[7] B. Zhang, X. Zheng, O. Voznyy, R. Comin, M. Bajdich, M. García-Melchor, L. Han, J. Xu, M. Liu, L. Zheng, F. P. García de Arquer, T. Dinh Cao, F. Fan, M. Yuan, E. Yassitepe, N. Chen, T. Regier, P. Liu, Y. Li, P. De Luna, A. Janmohamed, L. Xin Huolin, H. Yang, A. Vojvodic, H. Sargent Edward, *Science* **2016**, *352*, 333-337.

[8] T. Zhang, M. R. Nellist, L. J. Enman, J. Xiang, S. W. Boettcher, *ChemSusChem* **2019**, *12*, 2015-2021.

[9] L. Bai, S. Lee, X. Hu, *Angew. Chem. Int. Ed.* **2021**, *60*, 3095-3103.

[10] L. Trotochaud, S. L. Young, J. K. Ranney, S. W. Boettcher, *J. Am. Chem. Soc.* **2014**, *136*, 6744-6753.

[11] Y. Chen, K. Rui, J. Zhu, S. X. Dou, W. Sun, *Chem. Eur. J.* **2019**, *25*, 703-713.

[12] D. A. Corrigan, *J. Electrochem. Soc.* **1987**, *134*, 377.

[13] S. Anantharaj, S. Kundu, S. Noda, *Nano Energy* **2021**, *80*, 105514.

[14] M. S. Burke, S. Zou, L. J. Enman, J. Kellon, C. A. Gabor, E. Pledger, S. W. Boettcher, *J. Phys. Chem. Lett.* **2015**, *6*, 3737-3742.

[15] M. S. Burke, M. G. Kast, L. Trotochaud, A. M. Smith, S. W. Boettcher, *J. Am. Chem. Soc.* **2015**, *137*, 3638-3648.

[16] A. M. Smith, L. Trotochaud, M. S. Burke, S. W. Boettcher, *Chem. Commun.* **2015**, *51*, 5261-5263.

[17] D. Y. Chung, P. P. Lopes, P. Farinazzo Bergamo Dias Martins, H. He, T. Kawaguchi, P. Zapol, H. You, D. Tripkovic, D. Strmcnik, Y. Zhu, S. Seifert, S. Lee, V. R. Stamenkovic, N. M. Markovic, *Nature Energy* **2020**, *5*, 222-230.

[18] P. P. Lopes, D. Y. Chung, X. Rui, H. Zheng, H. He, P. Farinazzo Bergamo Dias Martins, D. Strmcnik, V. R. Stamenkovic, P. Zapol, J. F. Mitchell, R. F. Klie, N. M. Markovic, *J. Am. Chem. Soc.* **2021**, *143*, 2741-2750.

[19] R. Farhat, J. Dhainy, L. I. Halaoui, *ACS Catal.* **2019**, *10*, 20-35.

[20] C. Kuai, C. Xi, A. Hu, Y. Zhang, Z. Xu, D. Nordlund, C. J. Sun, C. A. Cadigan, R. M. Richards, L. Li, C. K. Dong, X. W. Du, F. Lin, *J. Am. Chem. Soc.* **2021**, *143*, 18519-18526.

[21] J. T. Mefford, X. Rong, A. M. Abakumov, W. G. Hardin, S. Dai, A. M. Kolpak, K. P. Johnston, K. J. Stevenson, *Nat. Commun.* **2016**, *7*, 11053.

[22] K. J. May, C. E. Carlton, K. A. Stoerzinger, M. Risch, J. Suntivich, Y. L. Lee, A. Grimaud, Y. Shao-Horn, *J. Phys. Chem. Lett.* **2012**, *3*, 3264-3270.

[23] L. J. Enman, M. B. Stevens, M. H. Dahan, M. R. Nellist, M. C. Toroker, S. W. Boettcher, *Angew. Chem., Int. Ed.* **2018**, *57*, 12840-12844.

[24] M. B. Stevens, C. D. M. Trang, L. J. Enman, J. Deng, S. W. Boettcher, *J. Am. Chem. Soc.* **2017**, *139*, 11361-11364.

[25] F. Dionigi, Z. Zeng, I. Sinev, T. Merzdorf, S. Deshpande, M. B. Lopez, S. Kunze, I. Zegkinoglou, H. Sarodnik, D. Fan, A. Bergmann, J. Drnec, J. F. d. Araujo, M. Gliech, D. Teschner, J. Zhu, W. X. Li, J. Greeley, B. R. Cuenya, P. Strasser, *Nat. Commun.* **2020**, *11*, 2522.

[26] F. Dionigi, P. Strasser, *Adv. Energy Mater.* **2016**, *6*, 1600621.

[27] J. O. Bockris, T. Otagawa, *J. Phys. Chem.* **1983**, *87*, 2960-2971.

[28] R. Subbaraman, D. Tripkovic, K. C. Chang, D. Strmcnik, A. P. Paulikas, P. Hirunsit, M. Chan, J. Greeley, V. Stamenkovic, N. M. Markovic, *Nat. Mater.* **2012**, *11*, 550-557.

[29] I. Spanos, M. F. Tesch, M. Yu, H. Tüysüz, J. Zhang, X. Feng, K. Müllen, R. Schlögl, A. K. Mechler, *ACS Catal.* **2019**, *9*, 8165-8170.

[30] R. Chen, S. F. Hung, D. Zhou, J. Gao, C. Yang, H. Tao, H. B. Yang, L. Zhang, L. Zhang, Q. Xiong, H. M. Chen, B. Liu, *Adv. Mater.* **2019**, *31*, 1903909.

[31] M. B. Stevens, L. J. Enman, A. S. Batchellor, M. R. Cosby, A. E. Vise, C. D. M. Trang, S. W. Boettcher, *Chem. Mater.* **2017**, *29*, 120-140.

[32] B. R. Wygant, K. Kawashima, C. B. Mullins, *ACS Energy Lett.* **2018**, *3*, 2956-2966.

[33] S. Jin, *ACS Energy Lett.* **2017**, *2*, 1937-1938.

[34] J. M. Ye, D. H. He, F. Li, Y. L. Li, J. B. He, *Chem Commun.* **2018**, *54*, 10116-10119.

[35] F. J. Sarabia, P. Sebastián-Pascual, M. T. M. Koper, V. Climent, J. M. Feliu, *ACS Appl. Mater. Interfaces* **2019**, *11*, 613-623.

[36] K. H. Gayer, A. B. Garrett, *J. Am. Chem. Soc.* **1949**, *71*, 2973-2975.

[37] W. Wilson's, *Comprehensive Analytical Chemistry. Volume 41. Sample Preparation for Trace Element Analysis, Vol. 41*, Elsevier, **2003**.